Accurate Calculation of Fringe Fields in the LHC Main Dipoles

S. Kurz
ITE, University of Stuttgart, Germany

S. Russenschuck, N. Siegel
CERN, Geneva, Switzerland

Abstract— **The ROXIE program developed at CERN for the design and optimization of the superconducting LHC magnets has been recently extended in a collaboration with the University of Stuttgart, Germany, with a field computation method based on the coupling between the boundary element (BEM) and the finite element (FEM) technique. This avoids the meshing of the coils and the air regions, and avoids the artificial far field boundary conditions. The method is therefore specially suited for the accurate calculation of fields in the superconducting magnets in which the field is dominated by the coil. We will present the fringe field calculations in both 2d and 3d geometries to evaluate the effect of connections and the cryostat on the field quality and the flux density to which auxiliary bus-bars are exposed.**

I. Introduction

The design and optimization of the LHC magnets is governed by the requirement of an extremely uniform field which is mainly defined by the layout of the superconducting coils. Even very small geometrical effects such as the keystoning of the cable, the insulation, grading of the current density in the cable due to different cable compaction and coil deformations due to collaring, cool down and electromagnetic forces have to be considered for the field calculation. For the field optimization of the LHC magnets [1], the usefulness of commercial software has shown to be limited in particular in the three dimensional case. Therefore the ROXIE [2] program package was developed at CERN for the design and optimization of the LHC superconducting magnets. Furthermore, the application of the BEM-FEM coupling method [3] yields the reduced field due to the magnetization of the iron yoke only. This avoids the meshing of the coils and the air regions, and avoids the artificial far field boundary conditions. The method is therefore specially suited for the calculation of fringe fields in the superconducting magnets, both in 2 and 3 dimensions.

II. The BEM-FEM Coupling Method

The total magnetic induction $\vec{B}$ in a certain point $\vec{\xi}$ in the aperture of the magnet can be decomposed into a contribution $\vec{B}_S$ due to the superconducting coil and a contribution $\vec{B}_R$ due to the magnetic yoke. If the fields are expressed in terms of the magnetic vector potential $\vec{B} = \operatorname{curl} \vec{A}$, then the decomposition into source and reduced contributions gives

$$\vec{A} = \vec{A}_S + \vec{A}_R. \tag{1}$$

This approach has the following intrinsic advantages:

- The coil field can be taken into account in terms of its source vector potential $\vec{A}_S$, which can be obtained easily from the filamentary currents I_S by means of Biot-Savart type integrals without meshing of the coil.
- The BEM-FEM coupling method allows a direct computation of the reduced vector potential $\vec{A}_R$ instead of the total vector potential $\vec{A}$. Consequently, numerical errors do not influence the dominating contribution $\vec{A}_S$ due to the superconducting coil.
- Since the field in the aperture is calculated through the integration over all the BEM elements, local field errors in the iron yoke cancel out and the calculated multipole content is sufficiently accurate even for a very sparse mesh.
- The surrounding air region need not be meshed at all. This simplifies the preprocessing and avoids artificial boundary conditions at some "far" distance. Since the air region is not meshed, only the iron region meshing is affected by geometrical modifications. This strongly supports the feature based, parametric geometry modelling which is required for mathematical optimization.

The elementary model problem for a single aperture model dipole (featuring both Dirichlet and Neumann bounds on the iron yoke) is shown in Fig. 1. When the

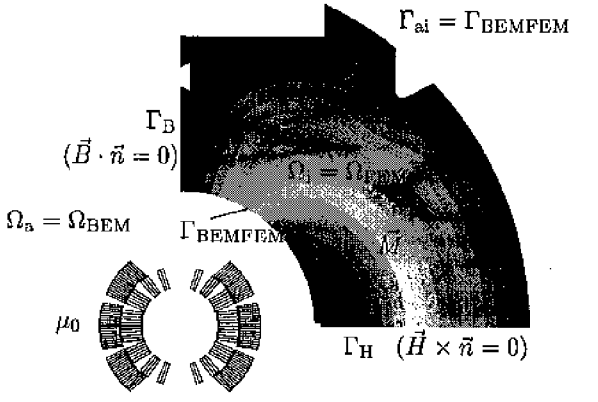

Fig. 1. Elementary model problem for the numerical field calculation of a superconducting (single aperture) model magnet. In the iron domain the total vector potential is displayed. The nonconductive air region Ω_a contains a certain number of conductor sources $\vec{J}$ which do not intersect the iron region Ω_i. The finite-element method inside the magnetic body $\Omega_i = \Omega_{FEM}$ is coupled with the boundary-element method in the domain outside the magnetic material $\Omega_a = \Omega_{BEM}$, by means of the normal derivative of the vector-potential on the interface $\Gamma_{ai} = \Gamma_{BEMFEM}$ between iron and air.

Manuscript received September 26, 1999

BEM-FEM coupling method is applied, only the magnetic sub-domain Ω_i which coincides with the magnetic yoke has to be meshed by finite elements. Iron saturation effects can then be treated within the FEM domain. The non-magnetic sub-domain Ω_a which represents the surrounding air region and the excitation coil is treated by the boundary element method. Only the common boundary Γ_{ai} needs to be discretized by boundary elements. If the domain Ω_i is discretized into finite elements (C^0-continuous, isoparametric 20-noded hexahedron elements are used), and the Galerkin method is applied to the weak formulation, then a non linear system of equations is obtained

$$\begin{pmatrix} [K_{\Omega_i\Omega_i}] & [K_{\Omega_i\Gamma_{ai}}] & 0 \\ [K_{\Gamma_{ai}\Omega_i}] & [K_{\Gamma_{ai}\Gamma_{ai}}] & [T] \end{pmatrix} \begin{pmatrix} \{\vec{A}_{\Omega_i}\} \\ \{\vec{A}_{\Gamma_{ai}}\} \\ \{\vec{Q}_{\Gamma_{ai}}\} \end{pmatrix} = \begin{pmatrix} 0 \\ 0 \end{pmatrix} \quad (2)$$

with all nodal values of $\vec{A}_{\Omega_i}$, $\vec{A}_{\Gamma_{ai}}$ and $\vec{Q}_{\Gamma_{ai}}$ grouped in arrays. As we will see later, $\vec{Q}_{\Gamma_{ai}}$ is the normal derivative of $\vec{A}$ on Γ_{ai}

$$\vec{Q}_{\Gamma_{ai}} = -\frac{\partial \vec{A}^{\mathrm{BEM}}_{\Gamma_{ai}}}{\partial n_a} \quad (3)$$

which we *assume* as given. The subscripts Γ_{ai} and Ω_i refer to nodes on the boundary and in the interior of the domain, respectively. The domain and boundary integrals in the weak formulation yield the stiffness matrices $[K]$ and the boundary matrix $[T]$. The stiffness matrices depend on the local permeability distribution in the nonlinear material. All the matrices in (2) are sparse. For the meshing of the boundary Γ_{ai} with boundary elements $\Gamma_{ai,j}$, C^0-continuous, isoparametric 8-noded quadrilateral boundary elements are used. The discrete analogue of the Fredholm integral equation can be obtained by successively putting the evaluation point $\vec{r}_0$ at the location of each nodal point $\vec{r}_j$. This procedure is called point-wise collocation and yields a linear system of equations,

$$[G]\{\vec{Q}_{\Gamma_{ai}}\} + [H]\{\vec{A}_{\Gamma_{ai}}\} = \{\vec{A}_s\}. \quad (4)$$

In (4), $\{\vec{A}_s\}$ contains the values of the source vector potential at the nodal points $\vec{r}_j, j = 1, 2, \ldots$. The matrices $[G]$ and $[H]$ are unsymmetric and fully populated. An overall numerical description of the field problem can be obtained by complementing the FEM description (2) by the BEM description (4) resulting in

$$\begin{pmatrix} [K_{\Omega_i\Omega_i}] & [K_{\Omega_i\Gamma_{ai}}] & 0 \\ [K_{\Gamma_{ai}\Omega_i}] & [K_{\Gamma_{ai}\Gamma_{ai}}] & [T] \\ 0 & [H] & [G] \end{pmatrix} \begin{pmatrix} \{\vec{A}_{\Omega_i}\} \\ \{\vec{A}_{\Gamma_{ai}}\} \\ \{\vec{Q}_{\Gamma_{ai}}\} \end{pmatrix} = \begin{pmatrix} 0 \\ 0 \\ \{\vec{A}_s\} \end{pmatrix} \quad (5)$$

Equation (4) gives exactly the missing relationship between the Dirichlet data $\{\vec{A}_{\Gamma_{ai}}\}$ and the Neumann data $\{\vec{Q}_{\Gamma_{ai}}\}$ on the boundary Γ_{ai}. It can be shown [4] that this procedure yields the correct physical interface conditions, the continuity of $\vec{n} \cdot \vec{B}$ and $\vec{n} \times \vec{H}$ across Γ_{ai}.

A detailed description of the method and the application to superconducting magnets can be found in [4], [5].

III. Field Quality in Accelerator Magnets

The magnetic field errors in the aperture of the magnets are expressed as the coefficients of the Fourier-series expansion of the radial field component at a given reference radius (in the 2-dimensional case). In the 3-dimensional case, the transverse field components are given at a longitudinal position z_0 or integrated over the entire length of the magnet. For a given radial component of the magnetic flux density B_r at a reference radius $r = r_0$ inside the aperture of a magnet the Fourier-series expansion of the field reads

$$B_r(r_0, \varphi) = \sum_{n=1}^{\infty} (B_n(r_0) \sin n\varphi + A_n(r_0) \cos n\varphi), \quad (6)$$

$$B_r(r_0, \varphi) = B_N(r_0) \sum_{n=1}^{\infty} (b_n(r_0) \sin n\varphi + a_n(r_0) \cos n\varphi), \quad (7)$$

with the main field component B_N ($N = 1$ dipole, $N = 2$ quadrupole, etc.). The B_n are called the *normal* and the A_n the *skew* components of the field given in Tesla, b_n the normal relative, and a_n the skew relative field components. They are dimensionless and are usually given in units of 10^{-4} at a 17 mm reference radius. In practice the B_r components are calculated in discrete points $\varphi_k = \frac{k\pi}{P} - \pi$, k =0,1,2,..,2P-1 in the interval $[-\pi, \pi)$ and a discrete Fourier transform is carried out:

$$A_n(r_0) \approx \frac{1}{P} \sum_{k=0}^{2P-1} B_r(r_0, \varphi_k) \cos n\varphi_k, \quad (8)$$

$$B_n(r_0) \approx \frac{1}{P} \sum_{k=0}^{2P-1} B_r(r_0, \varphi_k) \sin n\varphi_k. \quad (9)$$

The interpolation-error depends on the number of evaluation points and the amount of higher order multipole errors in the field. For the calculation of multipoles up to the order $n = 13$, 79 evaluation points ($P = 40$) are sufficient.

IV. Results

A. Field Quality in Collared Coils

Space limitations in the existing LEP tunnel and economical considerations have dictated a so-called *two-in-one* magnet design with two sets of coils and beam channels within a common mechanical structure, iron yoke, and cryostat. As a first example of the application of the BEM-FEM method we calculate the magnetic field in a configuration as shown in Fig. 2. Using double aperture stainless-steel collars with a relative permeability of $\mu_r = 1.0025$ creates asymmetries in the magnetic field in the case of warm measurements of the collared coil assembly where only one aperture is powered. The relative field errors at 17 mm reference radius in the aperture are given in Table 1. As was mentioned earlier the BEM-FEM method does not require the meshing of the coil (which can therefore be modelled with the required accuracy) and does not require a "far field" boundary condition which would influence considerably the results of this unbounded field problem.

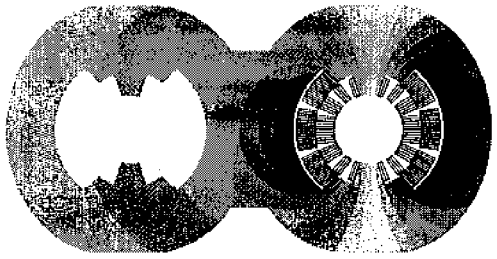

Fig. 2. Geometric model of one dipole coil powered for warm measurement in the combined collar structure assuming a constant relative permeability of $\mu_r = 1.0025$. The figure displays the magnetic flux density in the collars.

TABLE I

ADDITIONAL FIELD ERRORS IN COIL COLLAR ASSEMBLY WITH RIGHT-HAND-SIDE APERTURE POWERED FOR WARM MEASUREMENTS. (UNITS OF 10^{-4} AT 17 MM.) AND NOMINAL VALUES FOR A BARE COIL WITHOUT COLLAR.

Nominal				Additional			
b_2	0.0000	b_6	0.0000	b_2	-0.0737	b_6	0.0000
b_3	3.9150	b_7	0.7456	b_3	-1.6326	b_7	-0.0918
b_4	0.0000	b_8	0.0000	b_4	-0.0018	b_8	0.0000
b_5	-1.0385	b_9	0.1224	b_5	0.4306	b_9	0.0081

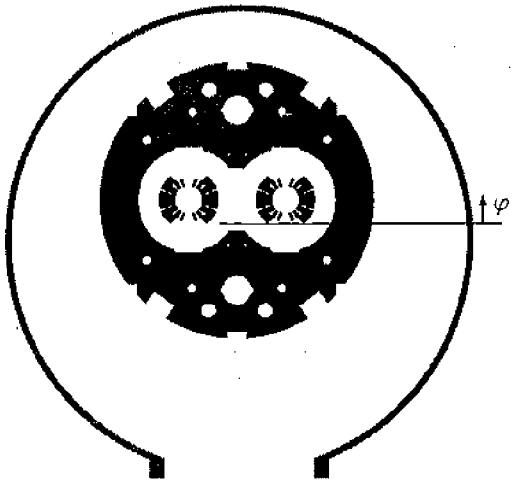

Fig. 3. Geometric model of the two-dimensional cross-section of the magnet showing iron yoke and cryostat vacuum vessel.

B. Influence of the Cryostat Eccentricity

The cold mass of the two-in-one magnet is placed in the vacuum vessel of the cryostat (made of magnetic steel) with an off-centering of 80 mm in the vertical plane, see Fig. 3. At the position of the support posts of the cold mass a circular opening is made in the cryostat vacuum vessel, closed by a non-magnetic plate. As a first approach, this opening has been modelled as a two-dimensional problem. The fringe field is higher at the opening but stays below $0.5 \cdot 10^{-3}$ Tesla, see Fig. 4. Again, the advantage of the BEM-FEM method lays in the fact that the surrounding air regions do not have to be considered and that the disconnected iron parts can be meshed independently with the required refinement. The eccentricity of the cryostat can therefore easily be modelled. Table 2 gives the nominal, and the additional field errors due to the cryostat at nominal field of 8.36 T in units of 10^{-4} at 17 mm.

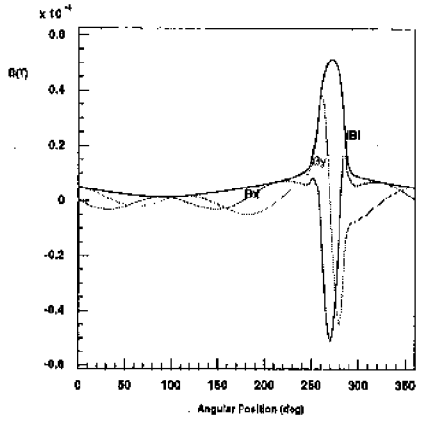

Fig. 4. Fringe field outside the vacuum vessel as a function of the angular position φ.

TABLE II

ADDITIONAL FIELD ERRORS DUE TO ASYMMETRY OF THE VACUUM VESSEL AT NOMINAL FIELD IN UNITS OF 10^{-4} AT 17 MM AND NOMINAL ERRORS FOR A COLD-MASS WITHOUT VACUUM VESSEL.

Nominal				Additional			
		a_1	0.000			a_1	0.422
b_2	0.646	a_2	0.000	b_2	0.099	a_2	-0.093
b_3	5.775	a_3	0.000	b_3	0.015	a_3	0.016
b_4	0.217	a_4	0.000	b_4	0.005	a_4	-0.002
b_5	-0.914	a_5	0.000	b_5	0.000	a_5	0.000

C. Fringe Field in the Coil-end Region

In order to reduce the peak field in the coil-end and thus increase the quench margin in the region with a weaker mechanical structure, the magnetic iron yoke ends approximately 80 mm from the onset of the coil-end at the non-connection side and about 300 mm from the onset of the coil-end at the connection end. This asymmetry results from the aim of a further reduction of the field in the ramp and splice region. The BEM-FEM coupling method is used for the calculation of the end-fields. In particular in 3D, the importance for not having to mesh the coil becomes obvious from Fig. 5. The ends can be modelled with the required

accuracy as the source field can be calculated directly by means of Biot-Savart's law. The two-in-one magnet end configuration with the common yoke used for the computation is shown in Fig. 6. Fig. 7 shows the field components

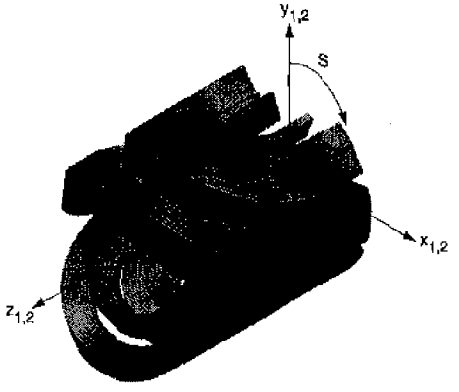

Fig. 5. Geometric model of the dipole coil-end with local coordinate system.

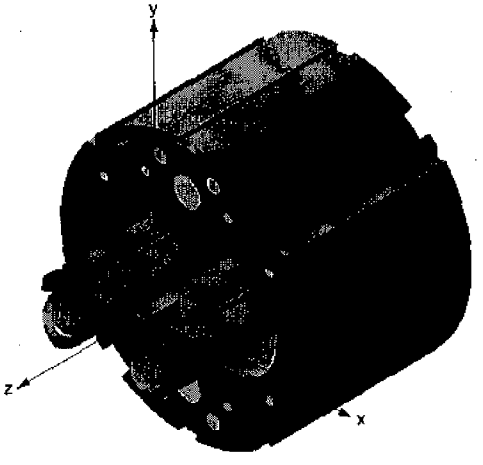

Fig. 6. Full 3D model of coils and two-in-one iron yoke. The location of the bus-bar is at x = 285 mm and y = -67 mm.

along a line in the end-region of the twin-aperture dipole prototype magnet (MBP2) from z = - 500 mm (inside the magnet yoke) to z = 400 mm outside the yoke. The onset of the coil-ends are at z = 0. On the non-connection side the iron yoke ends at z = -80 mm, on the connection side the iron yoke ends at z = -300 mm. This calculation is important for the evaluation of the forces acting on the 600 A and 6 kA auxiliary bus bars.

V. Conclusion

The BEM-FEM method is specially well suited for the calculation of fringe fields in superconducting magnets, as the coils and the air regions do not have to be represented in the finite-element mesh, discretization errors only influence the calculation of the yoke magnetization and there is not an artificial "far field" boundary condition. The method has been illustrated by three examples, the results of which

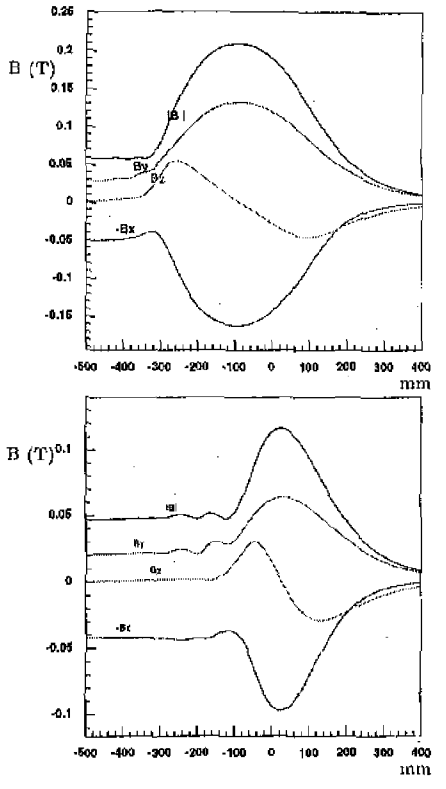

Fig. 7. Fringe field outside the dipole cold mass near the coil-end region, Top: connection end, Bottom: return end.

can be summarized as follows: 1) For warm measurements, an additional field error due to the stainless-steel collar of about -1.6 units in the relative b_3 component has to be considered. 2) The fringe field outside the cryostat stays below $5 \cdot 10^{-4}$ T and 3) the field seen by the 600 A and 6 kA auxiliary bus bars stays below 0.21 T in the coil-end region.

References

[1] The LHC study group. LHC, The Large Hadron Collider, Conceptual Design. *CERN/AC/95-05 (LHC)*, 1995.

[2] Editor: Stephan Russenschuck. ROXIE: Routine for the Optimization of magnet X-sections, Inverse field calculation and coil End design. *Yellow Report*, CERN 99-01(ISBN=92-9083-140-5), 1999.

[3] J. Fetzer, S. Abele, and G. Lehner. Die Kopplung der Randelementmethode und der Methode der finiten Elemente zur Lösung dreidimensionaler elektromagnetischer Feldprobleme auf unendlichem Grundgebiet. *Archiv für Elektrotechnik*, 76(5):361–368, 1993.

[4] S. Kurz, J. Fetzer, and W. Rucker. Coupled BEM-FEM methods for 3D field calculations with iron saturation. Proceedings of the First International ROXIE users meeting and workshop, 1999.

[5] S. Kurz and S. Russenschuck. The application of the BEM-FEM coupling method for the accurate calculation of fields in superconducting magnets. Accepted for publication in Electrical Engineering.